National Conference with International Participation

ENGINEERING MECHANICS 2008

Svratka, Czech Republic, May 12 – 15, 2008

FLOW ANALYSIS OF THE VORTEX SEPARATOR

P. Střasák[*], Z. Chára[**], B. Kysela [**]

Summary: *Numerical simulation of the flow in the vortex separator was performed by the program Fluent for two geometrical arrangements. The aim of the calculation was to estimate a particle separation efficiency for different particle size and density.*

1. Introduction

In a sewer system there are also present particles of non-organic origin, that have a negative impact on operating and maintenance of sewer systems and wastewater treatment works. Mainly in heavy rainfalls the load of solid particles is enormous and a removing of solids from urban water is desirable. Hydrodynamic vortex separator was firstly described by Smisson (1967) and now a variety of these devices can be found. They have no moving parts and they can be used directly in-line for preliminary and primary treatment at wastewater works or in a stand-by mode in the sewer systems. The flow inside the separators is very complex and therefore a CFD approach is widely used (Faram & Harwood, 2003). This contribution is focused on a CFD simulation of flow in a vortex separator and on a finding of particle removal efficiency for different particle sizes and densities.

2. Geometrical arrangements

Usually a tangential inflow pipeline is connected to a vortex separator in its lower part and/or in mid-chamber depth, this configuration is denoted here as separator B, see Fig. 1. Highly polluted water flows out as underflow and pre-treated water overflows in an upper part of the vortex separator into receiving waters. In this contribution we compare this traditional geometry with a new one, which is denoted as separator A, see Fig. 1. The inflow pipeline was connected to the vortex separator in its upper part. Inside the both separators there are water free levels. The diameter of the vortex separator was 8.4 m. depth 2.8 m, length of the overflow weir crest was 6.6 m, diameters of the inflow as well as outflow pipelines were 1.4, diameter of underflow pipe was 0.5 m. Hydraulic design parameters were as follows: design flow Q_d = 2 and 4 m^3/s, continuous underflow was constant Q_u = 0.22 m^3/s.

[*] Ing. Pavel Střasák, Ph.D.: TechSoft Engineering, spol. s r.o.. Táborská 31, Praha 4, tel. +420 261 102 303 fax: +420 261 102 273; e-mail: strasak@techsoft-eng.cz

[**] Ing. Zdeněk Chára, CSc.: Isntitute of Hydrodynamics AS CR, v. v. i., tel.: +420 233 109 011, fax: +420 233 324 361, e-mail: chara@ih.cas.cz

[**] Ing. Bohuš Kysela: Isntitute of Hydrodynamics AS CR, v. v. i., tel.: +420 233 109 011, fax: +420 233 324 361, e-mail: kysela@ih.cas.cz

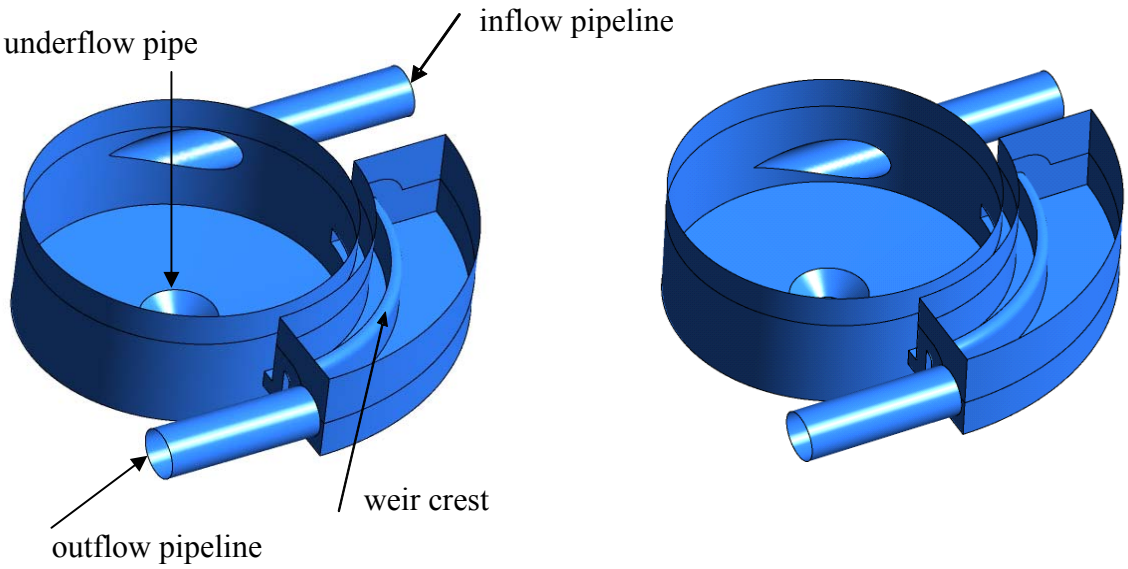

Fig. 1 Schematic views of the vortex separators

3. Numerical simulations

The numerical simulations were performed in the framework of the program Fluent 6.3. Firstly the outline of the separator was built, following by a meshing process. The total number of the computational cells was about 240000. The mesh consisted of 200000 hexahedrons and 40000 tetrahedrons. Picture of the final mesh is shown in Fig. 2. Several boundary conditions were applied. At the inlet there was a velocity inlet condition with constant velocity corresponding to the given flowrate (2 or 4 m^3/s). The underflow condition was modeled as mass flow rate with constant flow rate 220 kg/s. The condition at the outflow boundary was modeled as pressure outlet with a value of atmospheric pressure. The same condition was applied at the upper surface. Since the water free level is supposed inside the separator the flow was simulated as two phase flows (water and air) and the free surface was simulated by the VOF (Volume of Fluid) method. The flow was considered as unsteady and turbulent RNG k-ε model was applied.

To monitor the solids transportation two approaches can be used - Lagrangian particle tracking approach and Eulerian granular phase approach. In the first case discrete, non-interacting particles of defined size and density are released into the flow domain. This approach is applicable when solids concentrations are relatively low. In the second case the particulate phase is represented as a continuum of defined concentration and particle characteristics. Device efficiency is determined from knowledge of outlet concentrations compared to those at the inlet.

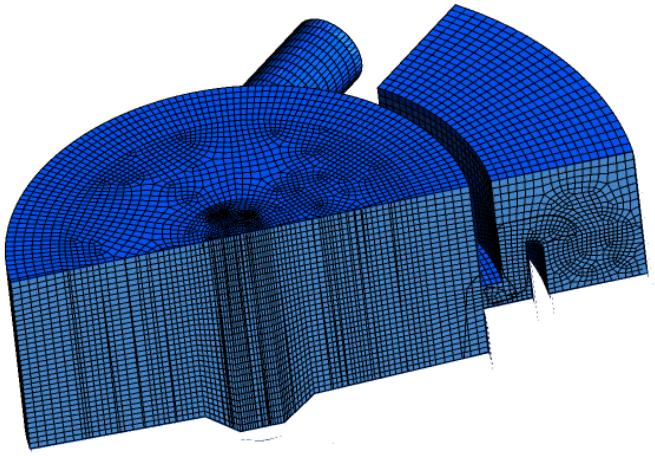

Fig. 2 Surface mesh

Discrete Phase Model (DPM) implemented in Fluent software is based on the Lagrangian approach. The trajectory of the discrete particle is calculated from the force balance on the particle, which is written in a Lagrangian reference frame. This force balance equates the particle inertia with the forces acting on the particle, and can be written (for the x direction in Cartesian coordinates) as

$$\frac{du_p}{dt} = F_D\left(u - u_p\right) + \frac{g_x\left(\rho_p - \rho\right)}{\rho_p} + F_x \tag{1}$$

where F_x is an additional acceleration (force/unit particle mass), term, $F_D(u\text{-}u_p)$ is the drag force per unit particle mass and

$$F_D = \frac{18\mu}{\rho_p\, d_p{}^2}\,\frac{C_D\,\mathrm{Re}_{rel}}{24} \tag{2}$$

Here, u is the fluid phase velocity, u_p is the particle velocity, μ is the dynamic viscosity of the fluid, ρ is the fluid density, ρ_p is the density of the particle, and d_p is the particle diameter. *Re* is the relative Reynolds number, which is defined as

$$\mathrm{Re} = \frac{\rho\, d_p \left|u - u_p\right|}{\mu} \tag{3}$$

The drag coefficient C_D is determined from the following relationship for smooth spherical particles (Morsi & Alexander, 1972)

$$C_D = a_1 + \frac{a_2}{\mathrm{Re}} + \frac{a_3}{\mathrm{Re}^2} \tag{4}$$

where a_1, a_2 and a_3 are constants depending on Reynolds number. For example in the range $10 < Re < 100$ the constants are: $a_1 = 0.6167$, $a_2 = 46.5$, $a_3 = -116.67$.

4. Results and discussion

As was mentioned above the numerical simulations were performed for two flowrates corresponding to the Reynolds numbers at the inlet pipeline 3.6×10^6 and 1.8×10^6, respectively. The simulations consisted of the steps. During the first step the calculations of velocity as well as free level position were carried out. In the second step the tracks of individual particles were monitored and analyzed. Shapes of the free level are shown in Fig. 3 for separator B for both flowrates.

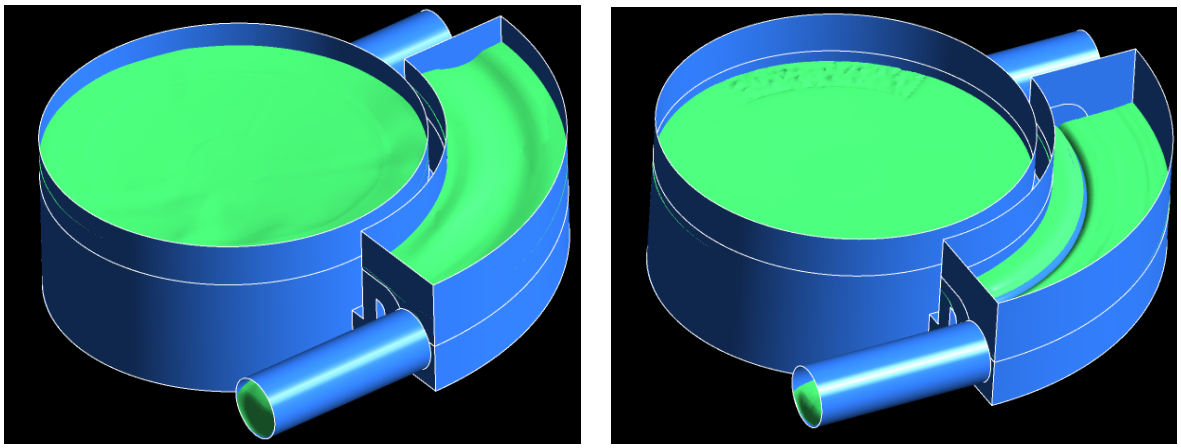

$Q_d = 4\ m^3/s$ $Q_d = 2\ m^3/s$

Fig. 3 Shapes of free levels, separator B

Inside the mean part of the separator we built a cylindrical surface with radius R=4.1 m on which the tangential component of the velocity field was recalculated. The resulting velocity vectors are displayed in Fig. 4 for separator A and in Fig. 5 for separator B, both for the flowrate $Q_d = 4\ m^3/s$.

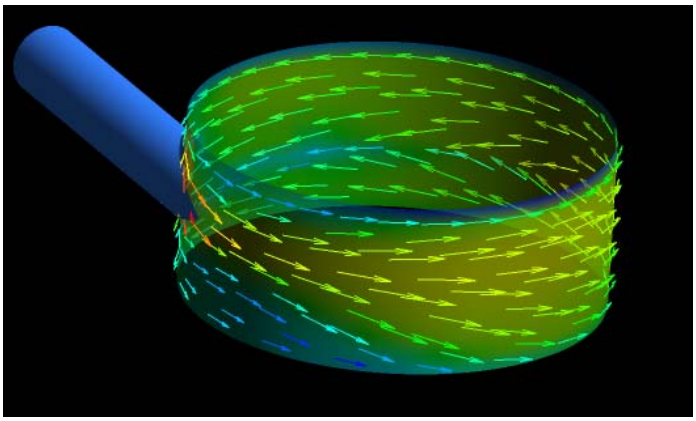

Fig. 4 Velocity vectors of tangential component on the surface R=4.1 m, separator A

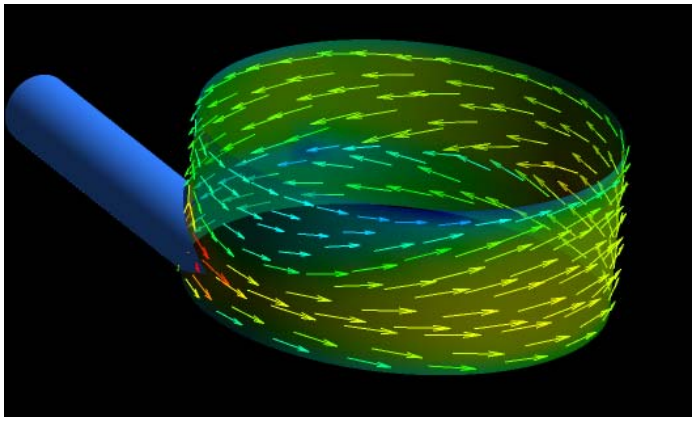

Fig. 5 Velocity vectors of tangential component on the surface R=4.1 m, separator B

While the velocity vectors have downward tendency in the separator A, see Fig. 4, on the contrary, in the separator B the velocity vectors have upward tendency to the free level.

When the velocity field was calculated individual particles were injected at the inlet profile. We analyzed several diameters of particles – 1, 2, 4 and 10 mm with different densities. In each run 213 particles were simultaneously injected. The removal efficiency was calculated as ratio of particles remaining in the separators to the all particles. The results are shown in Figs 6 and 7. In the case of the lower flowrate, Fig. 6, the removal efficiencies in both separators are more or less the same, except the particle of 2 mm, when the efficiency is somewhat better in the separator B. On the contrary, for the higher flowrate, Fig. 7, the efficiency in the separator A is always better for the particles of 1, 2 and 4 mm. According to our opinion it is due to the different flow patterns inside the separators, see Figs. 4 and 5.

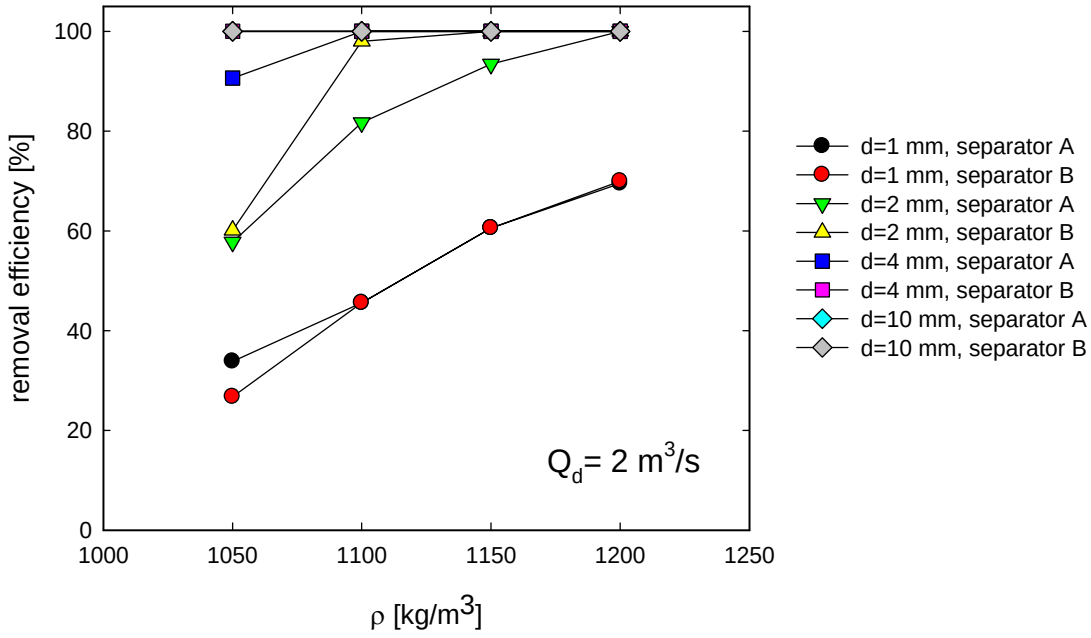

Fig. 6 Influence of particle size and densities on removal efficiency, $Q_d = 2\ m^3/s$

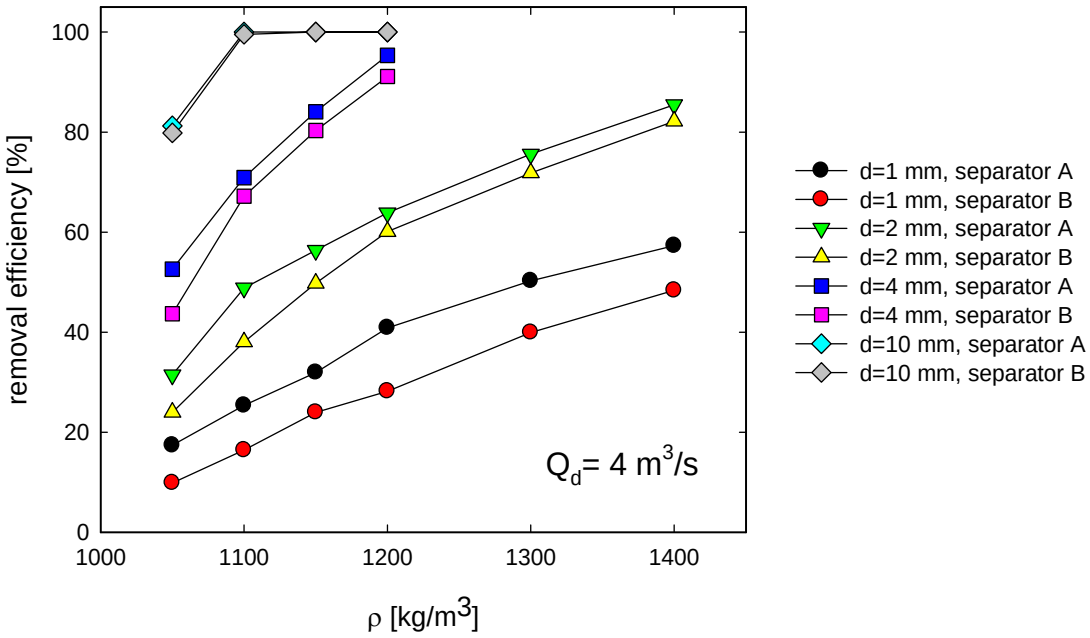

Fig. 7 Influence of particle size and densities on removal efficiency, $Q_d = 4\ m^3/s$

5. Conclusions

The numerical simulations were performed in the two separators. Instead of usual geometry of the flow inlet close to the separator bottom we tested the upper geometry. The simulations show that the upper geometry changes the flow inside the separator that results in better removal efficiency mainly for higher flow rates.

Acknowledgement

The paper will be partly supported by a Grant No IAA200600802 of the Grant Agency of the Academy of Sciences of the Czech Republic and Institutional Research Plan No. AV0Z20600510.

References

Faram, M.G. & Harwood, R. (2003) A method for the numerical assessment of sediment interceptors. Water Science and Technology, 47, 4, pp. 167-174.

Morsi, S. A. & A. J. Alexander, A. J. (1972) An Investigation of Particle Trajectories in Two-Phase Flow Systems. J. Fluid Mech., 55, 2, pp.193-208.

Smisson, B. (1967) Design, construction and performance of vortex overflows. Institution of Civil Engineers, Symposium on Storm Overflows, pp. 99-110.